Climatology of short-period mesospheric gravity waves over Halley, Antarctica (76°S, 27°W)

K. Nielsen [a,*,1], M.J. Taylor [a], R.E. Hibbins [b], M.J. Jarvis [b]

[a] Center for Atmospheric and Space Sciences and Physics Department, Utah State University, Logan, UT 84322, USA
[b] British Antarctic Survey, High Cross, Madingley Road, Cambridge, CB3 0ET, UK

A B S T R A C T

We present a first detailed climatological study of individual quasi-monochromatic mesospheric, short-period gravity-wave events observed over Antarctica. The measurements were made using an all-sky airglow imager located at Halley Station (76°S, 27°W) and encompass the 2000 and 2001 austral winter seasons. Distributions of wave parameters were found to be similar to findings at other latitudes. The wave headings exhibited unusually strong anisotropy with a dominant preference for motion towards the Antarctic continent and a rotation from westward during fall, to poleward in mid-winter, to eastward in spring. This rotation was accompanied by a systematic increase of ~50% in the magnitudes of the horizontal wavelengths and observed phase speeds. It is postulated that the observed wave anisotropy was due to a succession of wave sources of different characteristics lying equatorward of Halley, or a dominant source mechanism evolving with time during the winter months.

1. Introduction

It is now widely accepted that momentum deposition by short-period (<1 h) gravity waves plays a major role in the global meridional circulation at mesospheric heights (e.g., Fritts and Alexander, 2003). Global circulation models (GCM's) utilize significantly larger grid-sizes than the horizontal scales of these small-scale events (typical wavelengths 20–50 km), and currently their expected effects can only be incorporated into GCMs using (various) parameterization schemes. To better quantify small-scale wave effects, knowledge of their spatial characteristics, propagation, sources, and global distribution are of critical importance. All-sky nightglow imagers provide an exceptional opportunity for long-term studies of the temporal and horizontal spatial properties of these waves as they propagate upwards from their predominantly tropospheric sources.

Several climatology studies of short-period mesospheric gravity waves have already been performed, mainly from established field sites at mid-latitudes (e.g., Wu and Killeen, 1996; Walterscheid et al., 1999; Hecht et al., 2001; Stockwell and Lowe, 2001a; Ejiri et al., 2003), and at low-latitudes (e.g., Medeiros et al., 2003; Nakamura et al., 2003; Suzuki et al., 2004). Limited duration campaign measurements have also

provided important information on gravity-wave scale-sizes and propagation headings from less accessible, remote sites (e.g., Taylor et al., 1993, 1997; Hecht et al., 2004; Pautet et al., 2005). Together these measurements reveal similar ranges for the observed horizontal wavelengths and phase speeds of the wave events, regardless of their geographic origin in both the northern and southern hemispheres, suggesting a preponderance for similar-type tropospheric sources (such as deep convection), especially at mid- and low-latitudes. This result is illustrated in Table 1 which summarize average wave parameters from a number of imaging investigations worldwide.

While Table 1 shows that the average wave parameters are clearly in fair agreement (all yielding observed wave periods of less than 20 min), studies of their wave propagation headings show considerable site-to-site, latitudinal and seasonal variation. At mid-latitudes, Wu and Killeen (1996) were among the first to report a preferential eastward direction for short-period mesospheric gravity waves observed over a 14 month period from Peach Mountain Observatory, Michigan (42°N). Subsequently, Walterscheid et al. (1999) reported a dominant poleward motion for similar-type airglow wave events observed during the summer months from Adelaide, Australia (35°S), that appeared to switch over to mainly equatorward motion during the winter months (as determined from a more limited number of wave events). Further, mid-latitude measurements in the Northern Hemisphere from Urbana, Illinois (40°N) reported by Hecht et al., (2001) also revealed evidence for a predominant poleward motion during the spring and summer months (but no clear wave directionality was observed during the fall and winter seasons). Building on these

* Corresponding author.
E-mail address: knielsen73@gmail.com (K. Nielsen).
[1] Now at Computational Physics, Inc., 8001 Braddock Road Springfield, VA. 22151, USA.

Table 1

Summary results of several previous extended short-period gravity wave imaging studies at low- and mid-latitudes.

Observation site	Data duration (months)	λ_h (km)	c (m/s)	T (min)	Observed propagation direction	References
Rikubetsu, Japan 44°N	12	21–27	20–50	11	N–NE during summer changing to W during winter.	Ejiri et al. (2003)
Ontario, Canada 42°–43°N	5 (May–September)	25	45	10	Poleward with E zonal components during summer and W during winter.	Stockwell and Lowe (2001a)
Peach Mountain, MI, USA 42°N	14	N/A	N/A	N/A	Preferential eastward motion.	Wu and Killeen (1996)
Urbana, IL, USA 40°N	15	20–30	50	8	Poleward during spring and summer. No preference during fall and winter.	Hecht et al. (2001)
Nederland, CO, USA 40°N	3 (April–May)	N/A	24	N/A	Preferential N and E motion.	Taylor et al. (1993)
Shigaraki, Japan 35°N	12	21–27	20–50	11	N–NE during summer and SW during winter.	Ejiri et al. (2003)
Alcantara, Brazil 2°S	3 (September–October)	24	48	8	N–E during late spring/early summer.	Taylor et al. (1997)
Tanjungsari, Indonesia 7°S	12	13–45	37–75	9	Preferential poleward motion.	Nakamura et al. (2003)
Darwin, Australia 12°S	11	30–50	30–60	15	Poleward during summer, and both poleward and equatorward during winter.	Suzuki et al. (2004)
Wyndham, Australia 15°S	1 (November)	25–35	27–75	10	Poleward motion.	Pautet et al. (2005)
Cachoeira Paulista, Brazil 23°S	13	23	26	15	SE during summer, switching over to NW during winter.	Medeiros et al. (2003)
Adelaide, Australia 35°S	10	N/A	N/A	N/A	Poleward during summer and equatorward during winter.	Walterscheid et al. (1999)

results Ejiri et al., (2003) compared seasonal observations of the horizontal wave vectors observed from two stations in Japan, Shigaraki Observatory (35°N) and Rikubetsu (44°N) separated by only 9° in latitude, during summer months, the meridional component of wave propagation from both stations was poleward. However, only the southern-most station exhibited purely equatorward wave motions during the winter months while the northern-most station showed both poleward and equatorward motions. In contrast, the zonal components of wave propagation from both sites were found to exhibit a clear change over from eastward during summer months to westward motion in wintertime.

These results compare with more limited seasonal measurements at low-latitudes. Taylor et al. (1997) reported very strong wave directionality towards the northeast during the late spring/early summer (September–October) period for band-type wave events measured near the equator (2°S) during the NASA–INPE Guara Campaign conducted from Alcantara, Brazil. Subsequently, Medeiros et al. (2003) utilized one year of all-sky airglow measurements obtained from Cachoeira Paulista, Brazil (23°S) as part of a collaborative research program between INPE and Utah State University. During the summer months the wave motions over eastern Brazil were predominantly towards the southeast switching over to northwestward during winter months. Seasonal measurements at low-latitudes (12°S) have also been made from Darwin, Australia by Suzuki et al. (2004) demonstrating a clear poleward wave motion during the summer months, with both poleward and equatorward motions during the winter season, similar to the northern hemisphere mid-latitudes results of Ejiri et al. (2003).

A substantial fraction of the above results may be explained by the process of critical layer filtering of tropospheric gravity waves by the background wind field as they propagate up through the intervening atmosphere into the upper mesosphere. Critical layer filtering occurs when the background wind field in the direction of wave motion matches the observed phase speed (e.g., Hines and Reddy, 1967). In this situation, the intrinsic frequency of the wave is Doppler shifted to zero and the wave is absorbed into the background mean flow. Taylor et al. (1993) reported initial evidence of preferential directions for mesospheric gravity-wave propagation due to wind filtering in the middle atmosphere. They

computed polar plots, termed "blocking diagrams" that showed permitted, and blocked azimuths for wave propagation into the mesosphere assuming a climatologically wind field (Hedin et al., 1996) and a uniform distribution of tropospheric sources. The strong northward and eastward wave motions observed during three months of summer-time data from the Mountain Research Station in Colorado (40.0°N) (and by subsequent mid-latitude observers), were quite consistent with blocked azimuths resulting from wind-induced wave filtering at critical layers. Subsequently, Stockwell and Lowe (2001a,b) utilized airglow data from three stations in southwestern Ontario, Canada (42–43°N) and found that the dominant direction of wave propagation exhibiting an apparent rotation due to critical layer filtering caused by the seasonally changing background wind field (Stockwell and Lowe, 2001b).

However, other airglow data sets have also shown evidence for anisotropy in wave propagation headings mainly due to localization of the dominant wave sources. For example, the predominance for poleward directed wave motions observed over Indonesia (Tanjungsari, 7°S) by Nakamura et al. (2003), was most probably driven by the close proximity of strong convective sources that occur immediately to the north of Indonesia for most of the year. Similarly, during the Darwin Area Wave Experiment (DAWEX) campaign (October–December, 2001) Pautet et al. (2005) reported multiple events from Wyndham (15°S) in northern Australia that exhibited predominantly poleward (southward) wave motions, possible due to long-range ducted waves originating from the inter-tropical convergence zone (ITCZ) located over 1000 km to the north. Thus, both gravity-wave filtering and source anisotropy are expected to play key roles in the seasonal variability of mesospheric gravity waves, particularly at mid-latitudes where the stratospheric and mesospheric winds are strongest (e.g., Hedin et al., 1996).

In contrast, airglow image measurements of short-period gravity waves at high-latitudes are quite rare, mainly due to difficulties in making observations of the relative weak airglow emissions in comparison to the, at times, strong auroral emissions (e.g., Clairemidi et al., 1985; Taylor and Henriksen, 1989; Espy et al., 2004; Nielsen et al., 2006).
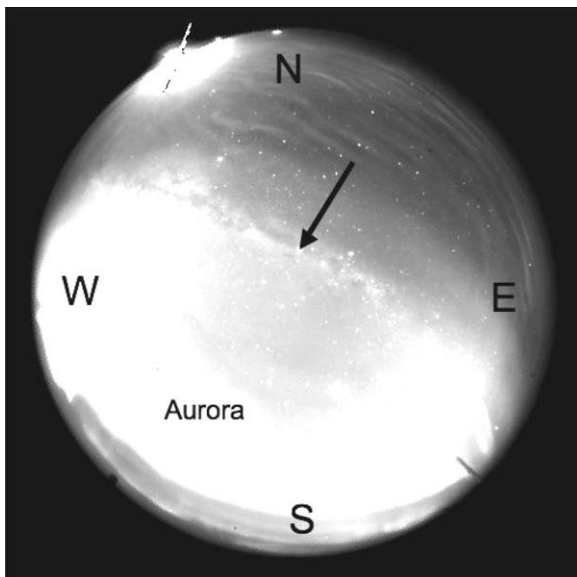
As part of a collaborative program with British Antarctic Survey, an all-sky airglow imager was installed at Halley,

Antarctica (76°S, 27°W) in 2000. The instrument was operated for two austral winter seasons before being moved to Rothera, Antarctica (68°S, 68°W). The primary goal of this program was to study the climatology of short-period gravity waves at southern polar latitudes during the winter months. A large number (>200) of extensive short-period events were observed during these two consecutive winter seasons exhibiting a marked anisotropy with the majority of the waves moving towards the Antarctic continent. Strong evidence for a systematic rotation in the preferred azimuthal wave propagation during the course of the season was also found. This study presents the first investigation of the seasonal climatology of individual quasi-monochromatic, short-period gravity-wave characteristics at high-southern latitudes.

2. Observations

Measurements of short-period, quasi-monochromatic gravity-wave events were made from Halley Station, Antarctica (76°S, 27°W) using an all-sky, multi-wavelength CCD imaging system. This is a well-proven field instrument similar in performance to the imager developed at USU under the National Science Foundation CEDAR program and successfully used to study gravity waves at low-, mid-, and high-northern latitudes (e.g., Taylor et al., 1997; Pautet et al., 2005; Nielsen et al., 2006). For our Antarctic measurements, sequential observations of the NIR OH (715–930 nm) and O_2 (865.5 nm) bands, and the Na (589.2 nm) emissions were made using exposure times of 15, 90 and 120 s, respectively, resulting in a cadence of ~2 min for the OH data and ~6 min for the other emissions. A background sky measurement at 572.5 nm was also regularly made to monitor cloud cover and auroral activity. Further details on the instrumentation are given in Taylor et al. (1997).

Fig. 1 shows an example of OH image displaying extensive short-period wave structure (termed bands) propagating towards the southwest, as indicated by the arrow. The data were obtained on June 4, 2000 during a period of moderate auroral activity, which can temporarily saturate the data (as evident in the lower part of the image), and illustrates some of the difficulties of imaging airglow structures at high-latitudes (e.g., Clairemidi et al., 1985; Nielsen et al., 2006). Nevertheless, successful airglow wave measurements were made from Halley throughout the austral winter periods (April–September) for two consecutive years, 2000 and 2001, resulting in a large number of distinct band-type wave events (total 221). These data have been analyzed to determine their observed (ground-reference) horizontal wave parameters (wavelength "λ_h", observed phase speed "c", observed period "T", and direction of propagation "φ") using well-established 2-D Fourier analysis methods (e.g., Garcia et al., 1997; Coble et al., 1998), and spatial mapping techniques. Typical uncertainties associated with these measurements are $\lambda_h \pm 1$ km, $c \pm 5$ m/s, $T \pm 1–2$ min and $\varphi \pm 5°$ (e.g., Taylor et al., 1997).

To investigate the intrinsic gravity-wave properties (as measured in a frame of reference moving with the background wind), we have utilized coincident mesospheric wind data obtained by a NOAA dynasonde co-located at Halley and operated as an imaging Doppler interferometer (Adams et al., 1985, 1986). This system has been described in detail elsewhere (Jones et al., 1997; Charles and Jones, 1999). Briefly, 2.75 MHz, 48 μs Gaussian pulse soundings were made on a log-periodic antenna every 5 min and signals returned from variations in the refractive index of the atmosphere were range-gated into 5 km bins between 50 and 105 km, although data presented herein are restricted to between 75 and 105 km from where the majority of echoes were returned. The location of each individual scattering point was then determined interferometrically after Doppler sorting of the echoes, and skymap locations and Doppler velocities of the scattering points were then used to fit a mean 3-dimensional velocity vector representative of the motion of the background neutral wind at a given altitude. Mean winds determined by a similar NOAA dynasonde using the same IDI technique have previously been calibrated against a meteor radar (Jones et al., 2003) and found to agree to within 10%, with the IDI returning consistently weaker winds than those recorded by the meteor radar over their common altitude range (80–95 km). Importantly, no systematic decrease in the agreement between the two techniques was observed with increasing height, and no statistically significant variation in the agreement between the two techniques was observed during day and night time operation.

Fig. 2 plots the zonal (a) and meridional (b) wind fields over Halley as measured by the IDI radar for the extended winter seasons of April to September, 2000 and 2001. The data are plotted as monthly averages with a temporal resolution of 1 h at 5 km intervals over the altitude range 75–105 km. The solid contour indicates the zero wind field line, while the dashed lines represent the 10 m/s contours. During the main winter months, the zonal wind field was predominantly eastward over the altitude range 75–90 km encompassing the nominal OH emission layer. The meridional wind field exhibited similar magnitude variations but with distinct semidiurnal signature. Both the zonal and meridional wind fields exhibited relatively low average wind speeds (<10 m/s) throughout the winter season (see also Hibbins et al., 2006, which shows wintertime mean winds below 10 m/s between 80 and 100 km). For the individual wave studies we have utilized hourly averaged wind data available with a height resolution of 5 km over the altitude range ~75–95 km.

Figs. 3 and 4 summarize the result of our image analyzes in the form of histogram plots of the observed wave parameters (Fig. 3) and their derived intrinsic distributions (Fig. 4). These data are plotted for the two winter seasons combined together, as separate analysis of the 2000 and 2001 data sets revealed no significant differences in their observed (and intrinsic) mean values or their distribution shapes. Fig. 3a shows that the majority of the quasi-monochromatic wave events exhibited horizontal wavelengths (λ_h) in the 15–40 km range with a mean value of ~26 km.
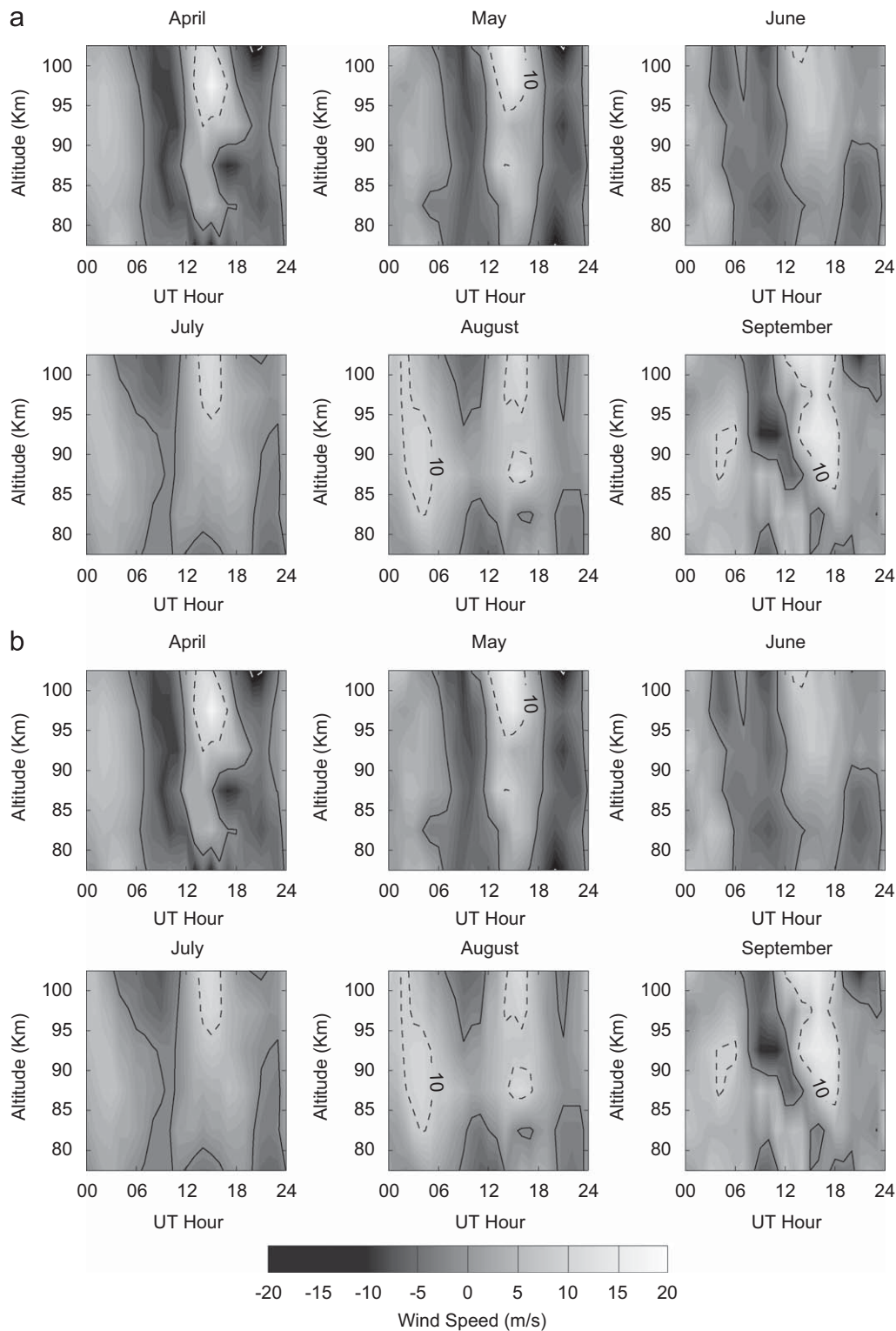

Fig. 1. All-sky image showing a short-period gravity wave over Halley in the OH emission on 4th June, 2000. The arrow indicates the direction of wave motion. Note the auroral activity in the lower part of image.

Fig. 2. Plots showing the hourly average zonal (a) and meridional (b) mean wind fields for each month during the observation campaign. The solid line indicates the zero wind contour while the dashed line represents the 10 m/s contour.

However, a significant number (~12%) exhibited longer wavelengths up to ~65 km. The observed horizontal phase speeds are shown in Fig. 3b and exhibit a more symmetric distribution ranging from ~10 to 100 m/s with typical values in the ~30–60 m/s range and an average value of ~48 m/s. The observed wave periods derived from these data are plotted in

Fig. 3c using 3 min wide bins and indicate a relatively sharp peak with a mean value of ~10 min and a typical range of 6–12 min (largest observed period ~33 min).

Using coincident hourly averaged IDI radar wind data, the intrinsic wave properties of 171 of the observed wave events were also determined. The intrinsic phase speed is defined as $c_i = c - u$,
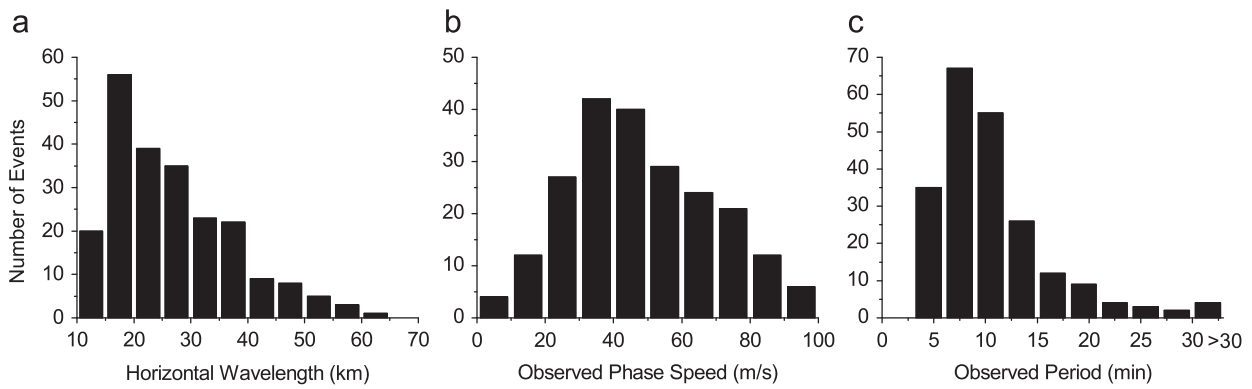
Fig. 3. Histogram plots showing the combined (2000 and 2001) distributions of observed wave parameters for the extended winter season at Halley.
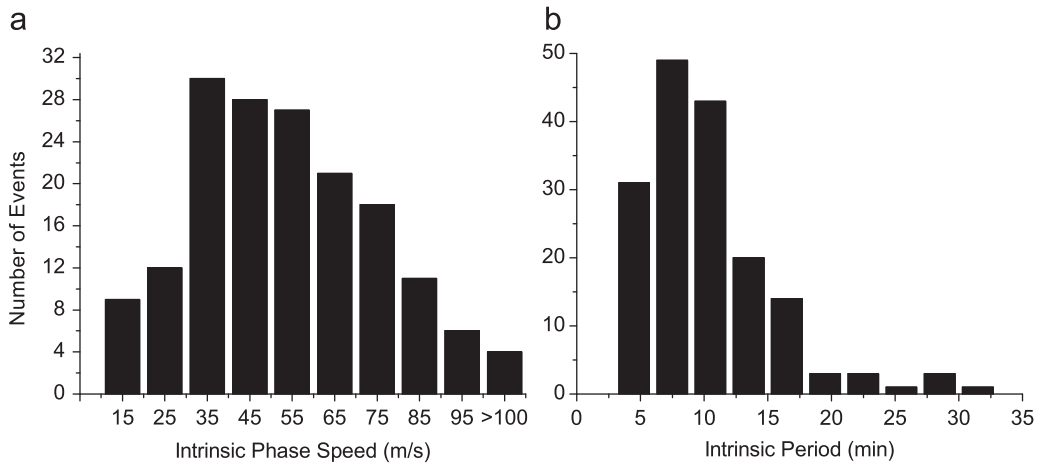

Fig. 4. Histogram plot of the derived intrinsic wave parameter distributions for the combined 2000 and 2001 observation seasons.

where u is the background wind in the direction of wave propagation, and the corresponding intrinsic period is $T_i = \lambda/c_i$. Fig. 4 plots the derived distributions of the waves' intrinsic phase speeds (a) and their corresponding intrinsic periods (b). (Note the horizontal wavelength of the wave events are not affected by the background winds.) Comparison with the observed wave distributions (Fig. 3b and c) reveals similar shapes and mean values for both the intrinsic phase speed and period distributions, with a mean intrinsic phase speed of ~52 m/s and an average intrinsic period of ~10 min. This is attributed to the fact that the mesospheric winds over Halley during the winter months were relatively weak, with typical values of $< \pm 10$ m/s (as illustrated in the radar summary plots of Fig. 2). Hence, in a climatological sense, the observed and intrinsic distributions were almost identical within the measurement uncertainties.

To investigate the horizontal azimuthal propagating characteristics, Fig. 5 plots the number of wave events versus their propagation direction (in 30° wide bins) for the combined 2000 and 2001 winter seasons comprising 150 events in 2000 and 71 in 2001. Note the smaller number of observed waves in 2001 was due to an instrument adjustment problem that restricted the quality observations to the early winter season (April–June). This format is similar to that used by previous researches to identify anisotropy in wave propagation headings (e.g., Taylor et al., 1997; Hecht et al., 2001; Ejiri et al., 2003; Nakamura et al., 2003). Fig. 5 reveals a remarkably strong preference for meridional wave propagation towards the Antarctic continent with majority of the events exhibiting a southward component of
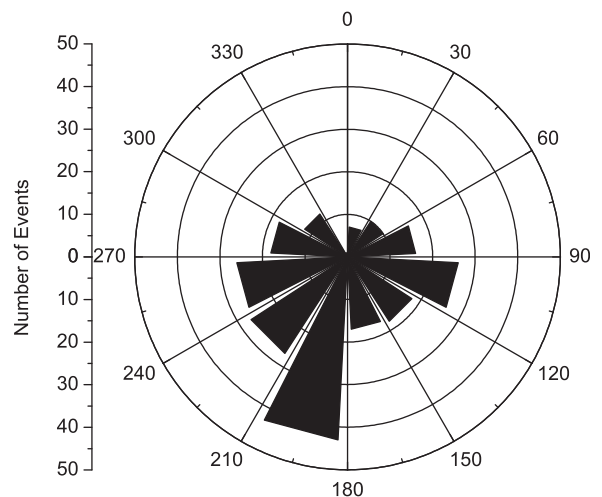

Fig. 5. Polar plot summarizing the 2000 and 2001 wave propagation headings. A clear preference for poleward propagating waves and a near absence of equatorward propagating events is evident.

motion throughout the winter time, distributed about a dominant, almost due poleward, wave direction (azimuth range 180–210°).

To investigate month-to-month variability in the wave propagation headings during the extended austral winter season, we
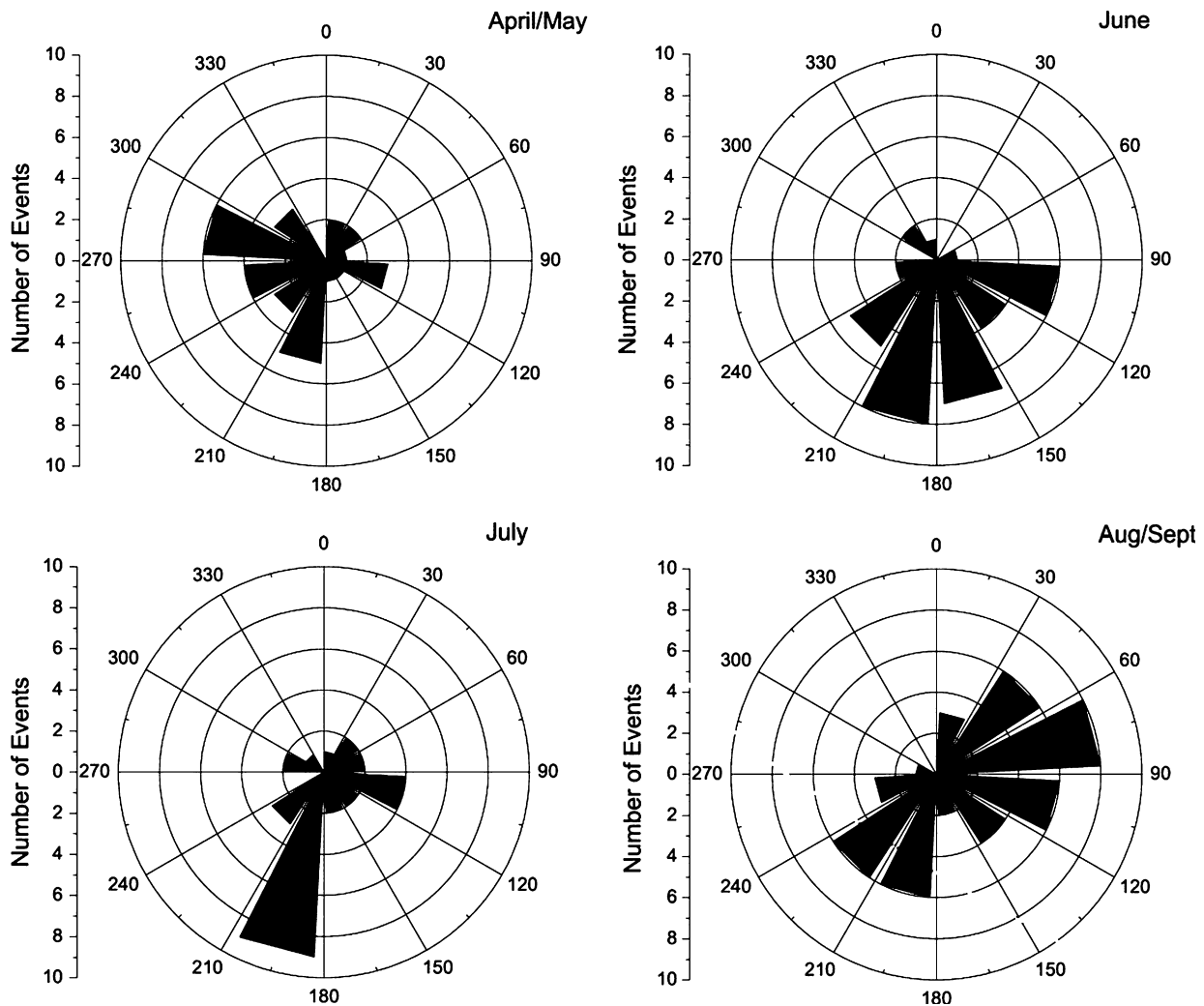
Fig. 6. Azimuthal plots of wave distribution as a function of the 2000 season. A clear rotation starting with northwest motion during fall (upper left) to poleward during the mid-winter months (June and July) and predominantly eastward during the spring period (lower right).

have divided the winter 2000 data set into four intervals, each comprising comparable number of events: April/May (41 events), June (36 events), July (28 events), and August/September (45 events). The data in April and September were sparse due to the shorter observation times available at the start and end of the season. The results are shown in Fig. 6 and reveal a very interesting behavior. During the austral fall period (April/May), the data exhibit a clear preference for westward zonal propagation with only limited meridional (north/south) motion. In comparison, June indicates a switch over to almost pure poleward (meridional) motion with roughly equal symmetry in the east–west components of motion. The wave directionality for July is even more remarkable and is dominated by strong, almost due poleward, propagation. Subsequently, the August/September data reveal a bi-polar distribution that is characterized by eastward zonal motion and almost equal preference for the meridional (north–south) wave components. Together, these data, strongly suggest a systematic counterclockwise rotation of wave propagation headings throughout the winter season, with predominantly westward waves during late fall changing to poleward wave motions throughout the deep winter months, and mainly eastward motion during the early spring period. Although the 2001 data set was limited in duration, it also exhibited a similar westward propagation during the austral fall period (not shown).

3. Discussion

These image measurements clearly establish the existence of copious amounts of short-period, quasi-monochromatic gravity waves in the high-latitude Antarctic mesosphere during the 6-month winter season. The spatial and temporal morphologies of these wave events (λ_{h}, c, T) and their observed distributions as measured from Halley are similar in their respective mean values and typical ranges when compared with mesospheric gravity-wave observations from numerous other sites at mid- and low-latitudes in both hemispheres (e.g., Taylor et al., 1997; Stockwell and Lowe, 2001a; Ejiri et al., 2003; Medeiros et al., 2003; Nakamura et al., 2003; Hecht et al., 2004; Suzuki et al., 2004; Pautet et al., 2005). Together, these data help establish the global presence of copious short-period gravity waves.

In contrast, the strong anisotropy evident in the wave propagation headings (Fig. 5) as observed from Halley during 2000 (and 2001) is quite different from that evident from an ensemble of airglow wave measurements from other lower latitude sites (as summarized in Table 1) which show a seasonal switch over in their meridional direction of motion from summer to wintertime. As discussed earlier, Walterscheid et al. (1999) identified this change over using airglow image data from southern Australia. They determined that during the summer months, small-scale gravity waves were predominantly poleward
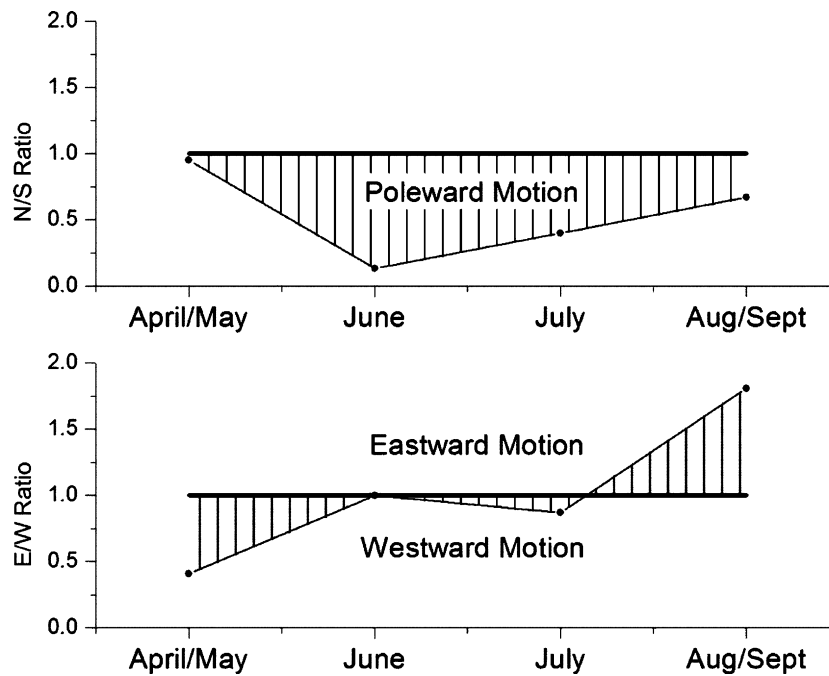
Fig. 7. The top panel shows the ratio between north/south wave propagation while the lower panel illustrates the ratio between the zonal components (east/west).

propagating, while during winter their motions were mainly equatorward. Additional evidence in support of this seasonal switch over from poleward to equatorward in the meridional component of the wave motions has since been obtained from several sites in North- and South America, Japan, and Australia encompassing both hemispheres (e.g., Taylor et al., 1997; Stockwell and Lowe, 2001b; Ejiri et al., 2003; Medeiros et al., 2003; Nakamura et al., 2003; Hecht et al., 2004; Suzuki et al., 2004; Pautet et al., 2005). In stark contrast, our Antarctic data show a marked preference for poleward meridional wave motion during the winter months, opposite to that observed at lower latitudes, and in addition, a clear rotation of the zonal component of the wave motions from west to east during the course of the winter.

The observed rotation of the wave azimuths at Halley is a most unusual result. It was first reported in the momentum flux derivations of Espy et al. (2004) which were obtained using Na imagery (recorded at the same time as the OH data), but integrated across the gravity-wave spectrum. Here this rotation is clearly evident in the propagation direction distributions derived from analyzing individual, quasi-monochromatic wave events throughout the 2000 (and 2001) winter seasons. Unfortunately, airglow measurement techniques are limited to observations under dark sky conditions and there are no summer-time data available to further investigate the seasonal variability in the wave headings. However, a new technique to detect gravity waves in the D region ionosphere using an imaging riometer is currently being investigated for year-round gravity-wave studies at Halley (Jarvis et al., 2003; Moffat-Griffin et al., 2008). What is clear from our wintertime measurements is that the fall and spring periods (Fig. 6) show a distinct change in the zonal wave motions from westward to eastward respectively with dominant poleward zonal motion throughout the winter season. This result is investigated further in Fig. 7, which divides the wave data of Fig. 6 into their meridional and zonal components and plots separately the ratio of the number of north/south events and east/west events during the period April through to September. The upper panel (plot a) shows the dominant poleward motion throughout this 6-month period while the lower panel (plot b) illustrates the systematic switch

over from westward motion during the fall to eastward motion in the spring. The accompanying effects of this rotation on the observed wave parameters are illustrated in Fig. 8 which presents the horizontal wavelength (plot a), observed phase speed (plot b), and observed period (plot c) as a function of azimuth for all 150 wave events observed during the 2000 winter period. Combining this information with our knowledge of the rotation of the wave vectors from month-to-month, it is evident that during the fall (April/May) period the horizontal wavelengths were relatively short (mean $\sim$20 km) while their observed phase speeds were also low ($\sim$30 m/s) and were directed predominantly westward. During the peak winter months (June/July) when strong poleward motion occurred, the horizontal wavelengths and the observed phase speeds both increased substantially to around $\sim$30 km and $\sim$50 m/s, respectively. The wave events observed subsequently during the spring period (August/September) also exhibited high values for their horizontal wavelengths and observed phase speeds. One consequence of this unusual behavior is illustrated in plot c which shows very little change in the observed period ($= \lambda_h/c$) which remained $<$20 min for all but a few ($<$6%) of the 150 events recorded during this $\sim$6 month observing period.

To better appreciate the systematic changes in magnitude of the observed wave parameters with season (and hence azimuth), Fig. 9 plots the horizontal wavelength (top panel) and the observed phase speed (bottom panel) as a function of day of year. The data points appear in clusters due to several limiting factors including no observations during full moon intervals and extensive cloud cover, which tended to span several days. The solid lines in each plot are quadratic fits to the data and show that the mean horizontal wavelength systematically changed from $\sim$20 to 30 km ($\sim$50% increase), while the observed phase speeds experienced a similar type increase from $\sim$30 to $\sim$50 m/s. In summary, Figs. 8 and 9 clearly reveal a significant seasonal asymmetry in the wave parameters (λ_h, c), as the horizontal wavelength and the observed phase speed both systematically increased in magnitude during the course of the extended Antarctic winter period.

a

b

c
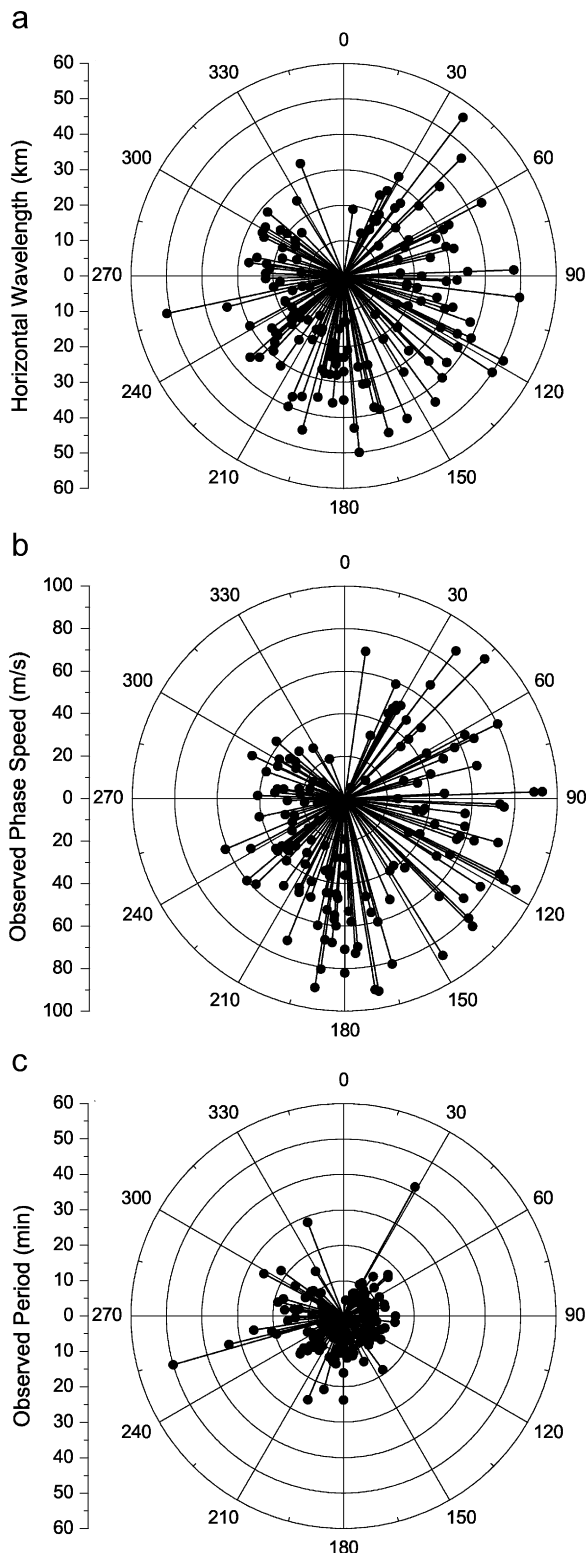
Fig. 8. Plots illustrating the variation in the observed wave parameters with azimuth for the 2000 season. The top two panels show the variation of horizontal wavelengths (observed phase speeds) with smaller wavelengths (phase speeds) dominating the westward motion while eastward motion was characterized by longer wavelengths (and higher phase speeds). The bottom panel shows the observed period, which remained fairly constant with azimuth.

Some of the above results are qualitatively consistent with critical layer filtering of the waves by seasonal variations in the background wind field. As described earlier, critical layer filtering


a

b
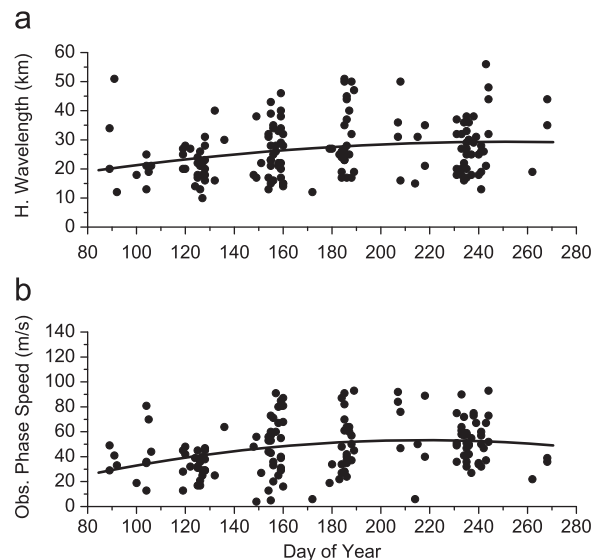
Fig. 9. Scatter plot of horizontal wavelength (top) and observed phase speed (bottom) as a function of day of year. The solid line indicates a quadratic fit to the two data sets.

occurs when the background wind field in the direction of wave motion matches the observed phase speed and the wave is absorbed into the background mean flow (e.g., Hines and Reddy, 1967). This mechanism can impose marked anisotropy in the observed seasonal wave distributions particularly at mid-latitudes where the zonal stratospheric and mesospheric winds are strongest.

Unfortunately, measurements of the stratospheric and lower mesospheric wind fields are rare at any site and not available at Halley. In concert with other recent studies we have therefore used climatological wind information as given by the HWM-93 model (Hedin et al., 1996) to investigate potential effects of critical layer filtering over Halley. In addition, we have also utilized coincident IDI wind data from Halley to investigate potential wind effects within the airglow region and it's near vicinity.

During the Antarctic winter months the wind field in the middle atmosphere is primarily eastward, dominated by the strong Antarctic wind jet near 50 km, with climatological magnitudes up to ~40 m/s. The expected effect of this jet on an initially isotropic wave field is illustrated in Fig. 10, which plots the observed phase speeds versus azimuth for the combined 2000 and 2001 data sets. The shaded circular area to the east of the center represents the maximum expected blocking region throughout the observed winter period. Our results suggest that during the early winter season, the observed wave phase speeds are relatively low (<40 m/s) and mainly westward. The blocking region to the east will filter out such waves and can account for the apparent absence of low phase speed waves propagating eastward. However, climatological wind filtering alone cannot account for the distinct lack of meridional wave propagation during this period. Similarly, during the main winter months (June/July), wind filtering may account for the low number of eastward propagating waves, but it provides no evidence of supporting the observed lack of westward propagating waves and the continued absence of equatorward propagating waves. Finally, during the latter part of the winter, the observed wave phase speeds were eastward and of significantly larger magnitude than earlier in the season. Wind filtering provides an adequate explanation for the absence of low phase speed eastward waves, resulting in the observed predominance for high phase speed waves during this period. However, it cannot account for the observed bi-polar wave propagation as evident in Fig. 6.
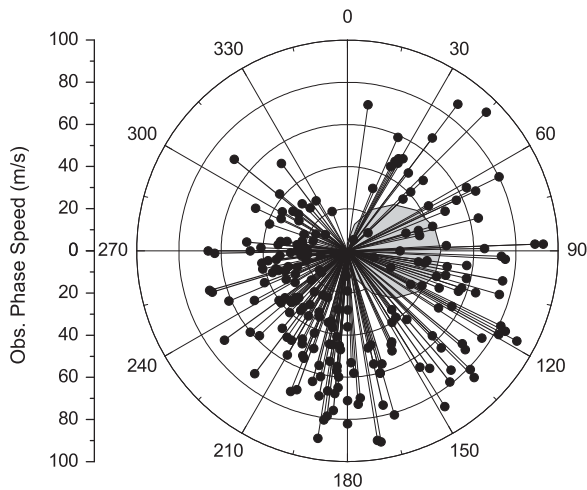
Fig. 10. Plot summarizing the expected effects of critical layer filtering on the observed wave propagation anisotropy for the combined 2000 and 2001 seasons. The observed phase speed is plotted versus wave azimuth while the shaded area indicates the region of climatological wind filtering. While wind filtering may account for the lack of slow phase speed waves (<40 m/s) propagating eastward, it does not account for the observed strong poleward wave motions during mid-winter and the systematic increase in the magnitudes of the horizontal wavelengths and observed phase speed with time.

Thus, although critical wave filtering by the strong Antarctic wind jet near 50 km is partly capable of explaining our observations, there remain important differences that require other explanations. These are the complete lack of equatorward wave motion throughout the winter season, the absence of high phase speed waves in the early winter months (April/May), and the subsequent decrease in the number of westward propagating waves giving rise to an apparent rotation in the wave field. The observed systematic increases in the horizontal wavelengths and wave phase speeds are also problematic.

Strong upper mesospheric tidal winds have also been shown capable of causing an anisotropic wave field due to filtering effects (Stockwell and Lowe, 2001b). To further understand the expected influence of tidal variability at mesospheric heights, we have also considered the effects of the measured wind field within the airglow region. The majority of the observed wave events were observed between 21 and 03 UT (not shown), and thus experienced both phases of the meridional semidiurnal tidal wind which exhibited a monthly average amplitude of <10 m/s (as shown in Fig. 2). Although the instantaneous tidal wind amplitudes are expected to be of significantly larger amplitude, the relative high observed phase speeds of the waves (average ~50 m/s) suggest that mesospheric tidal wind variability was probably not the source of the observed anisotropy.

In summary, the apparent lack of a dominant wind filtering signature suggests that significant anisotropy in the geographical distribution of the wave sources existed. In particular, the rotation of the wave azimuths and the evolution of the wave distribution during the extended winter season strongly suggest either a succession of wave sources of different characteristics, or the intriguing possibility of a dominant source mechanism that evolved with time during the winter months (or a combination thereof). The combination of a complete lack of waves propagating equatorward and Halley being situated on the Antarctic coast concludes that the region poleward of Halley is a weak wave generator and suggest that the most likely source(s) of the observed waves resides to the north over the Weddell Sea. Possible candidate sources are orographic forcing by mountains and katabatic winds blowing across the ice shelf (Wu and Jiang,

2002; Watanabe et al., 2006), unbalanced flow in mesoscale cyclones termed "polar lows", which frequently occur over the Weddell Sea, the polar vortex (Ratnam et al., 2004; Yoshiki et al., 2004), the polar night jet (Yoshiki and Sato, 2000; Hei et al., 2008), and the auroral electrojet (Chimonas and Hines, 1970), To investigate these potential wave sources it is also necessary to know the nature of the wave propagation (e.g., free propagating, ducted, or evanescent wave events). In particular, Taylor et al. (1997), Walterscheid et al. (1999), Hecht et al. (2001), Suzuki et al. (2004), and Pautet et al. (2005) have observed ducted short-period gravity waves capable of propagating large distances (>1000 km) from their source regions. While the dominant source(s) of the short-period waves observed over Halley are expected to be associated with cyclonic activity over the Weddell Sea, they are not yet known and are currently under investigation.

4. Summary

An all-sky airglow imager has been used to obtain novel data on the climatology of short-period mesospheric gravity waves over Halley, Antarctica. This study provides the first seasonal investigation of these waves at high Antarctic latitudes. Measurements were obtained during the austral winter over a two-year period (2000 and 2001). The distribution of observed wave parameters (λ_h, c, T_{ob}) were essentially identical to previous measurements of similar-type small-scale waves at low- and mid-latitudes. Strong seasonal variability in the wave propagation directions was observed especially during the 2000 season with a marked preferential westward motion during the fall period changing to strong poleward motion during the main winter months and eastward motion during the spring period.

Comparison with the climatological wind field suggests that the observed systematic variation in the magnitude of the wave parameters and their direction of motion are most probably not due to wind filtering effects alone. Instead, we postulate that this unusual rotation of the wave headings may have arisen from a source region located to the north of Halley that evolved significantly in its characteristic during the winter season (or a succession of such sources generating different wave characteristics). The most probable sources are associated with strong cyclonic activity over the Weddell Sea but other potential sources are under investigation.

Acknowledgments

References

Adams, G.W., Edwards, D.P., Brosnahan, J.W., 1985. The imaging Doppler interferometer—data analysis. Radio Sci. 20 (6), 1481–1492.

Adams, G.W., Brosnahan, J.W., Walden, D.C., Nerney, S.F., 1986. Mesospheric observations using a 2.66-MHz radar as an imaging Doppler interferometer—description and 1st results. J. Geophys. Res. 91 (A2), 1671–1683.

Charles, K., Jones, G.O.L., 1999. Mesospheric mean winds and tides observed by the imaging Doppler interferometer (IDI) at Halley, Antarctica. J. Atmos. Terr. Phys. 61 (5), 351–362.

Chimonas, G., Hines, C.O., 1970. Atmospheric gravity waves launched by auroral currents. Planet. Space Sci. 18, 565–582.

Clairemidi, J., Hersé, M., Moreels, G., 1985. Bi-dimensional observations of waves near the mesopause at auroral latitudes. Planet. Space Sci. 33, 1013–1022.

Coble, M.R., Papen, C., Gardner, C.S., 1998. Computing two-dimensional unambiguous horizontal wavenumber spectra from OH airglow images. IEEE Trans. Geosci. Remote Sensing 36, 368–382.

Ejiri, M.K., Shiokawa, K., Ogawa, T., Igarashi, K., Nakamura, T., Tsuda, T., 2003. Statistical study of short-period gravity waves in OH and OI nightglow images at two separated sites. J. Geophys. Res. 108 (D21), 4679.

Espy, P.J., Jones, G.O.L., Swenson, G.R., Tang, J., Taylor, M.J., 2004. Seasonal variations of the gravity wave momentum flux in the Antarctic mesosphere and lower thermosphere. J. Geophys. Res. 109, D23109.

Fritts, D.C., Alexander, M.J., 2003. Gravity wave dynamics and effects in the middle atmosphere. Rev. Geophys. 41.

Garcia, F.J., Taylor, M.J., Kelley, M.C., 1997. Two-dimensional spectral analysis of mesospheric airglow image data. Appl. Opt. 36, 7374–7385.

Hecht, J.H., Walterscheid, R.L., Hickey, M.P., Franke, S.J., 2001. Climatology and modeling of quasi-monochromatic atmospheric gravity waves observed over Urbana Illinois. J. Geophys. Res. 106 (D6), 5181–5195.

Hecht, J.H., Kovalam, S., May, P.T., Mills, G., Vincent, R.A., Walterscheid, R.L., Woithe, J., 2004. Airglow imager observations of atmospheric gravity waves at Alice Springs and Adelaide, Australia during the Darwin Area Wave Experiment (DAWEX). J. Geophys. Res. 109, D20S05.

Hedin, A.E., Fleming, E.L., Manson, A.H., Schmidlin, F.J., Avera, S.K., Clark, R.R., Franke, S.J., Fraser, G.J., Tsuda, T., Vial, F., Vincent, R.A., 1996. Empirical wind model for the upper, middle and lower atmosphere. J. Atmos. Sol. Terr. Phys. 58, 1421–1447.

Hei, H., Tsuda, T., Hirooka, T., 2008. Characteristics of atmospheric gravity wave activity in the polar regions revealed by GPS radio occultation data with CHAMP. J. Geophys. Res. 113, D04107.

Hibbins, R.E., Espy, P.J., Jarvis, M.J., 2006. Mean winds and tides in the mesosphere and lower thermosphere above Halley, Antarctica. J. Atmos. Sol. Terr. Phys. 68, 436–444.

Hines, C.O., Reddy, C.A., 1967. On the propagation of atmospheric gravity waves through regions of wind shear. J. Geophys. Res. 72, 1015–1034.

Jarvis, M.J., Hibbins, R.E., Taylor, M.J., Rosenberg, T.J., 2003. Utilizing riometry to observe gravity waves in the sunlit mesosphere. Geophys. Res. Lett. 30 (19), 1979.

Jones, G.O.L., Charles, K., Jarvis, M.J., 1997. First mesospheric observations using an imaging Doppler interferometer adaptation of the dynasonde at Halley, Antarctica. Radio Sci. 32 (6), 2109–2122.

Jones, G.O.L., Berkey, F.T., Fish, C.S., Hocking, W.K., Taylor, M.J., 2003. Validation of imaging Doppler interferometer winds using meteor radar. Geophys. Res. Lett. 30 (14), 1743.

Medeiros, A.F., Taylor, M.J., Takahashi, H., Batista, P.P., Gobbi, D., 2003. An investigation of gravity wave activity in the low-latitude upper mesosphere: propagation direction and wind filtering. J. Geophys. Res. 108 (D14), 4411.

Moffat-Griffin, T., Hibbins, R.E., Nielsen, K., Jarvis, M.J., Taylor, M.J., 2008. Observing mesospheric gravity waves with an imaging riometer. J. Atmos. Sol. Terr. Phys.

Nakamura, T., Aono, T., Tsuda, T., Admiranto, A.G., Achmad, E., Suranto, 2003. Mesospheric gravity waves over a tropical convective region observed by OH airglow imaging in Indonesia. Geophys. Res. Lett. 30 (17), 1882.

Nielsen, K., Taylor, M.J., Pautet, P.-D., Fritts, D.C., Mitchell, N., Beldon, C., Williams, B.P., Singer, W., Schmidlin, F.J., Goldberg, R.A., 2006. Propagation of short-period gravity waves at high-latitudes during the MaCWAVE winter campaign. Ann. Geophys. 24, 1227–1243 SRef_ID:1432-0576/ag/2006-24-1227.

Pautet, P.-D., Taylor, M.J., Liu, A.Z., Swenson, G.R., 2005. Climatology of short-period gravity waves observed over northern Australia during the Darwin area wave experiment (DAWEX) and their dominant source regions. J. Geophys. Res. 110, D03S90.

Ratnam, M.V., Tsuda, T., Jacobi, C., Aoyama, Y., 2004. Enhancement of gravity wave activity observed during a major Southern Hemisphere stratospheric warming by CHAMP/GPS measurements. Geophys. Res. Lett. 31, L16101.

Stockwell, R.G., Lowe, R.P., 2001a. Airglow imaging of gravity waves 1. Results from a small network of OH nightglow scanning imagers. J. Geophys. Res. 106 (D15), 17185–17203.

Stockwell, R.G., Lowe, R.P., 2001b. Airglow imaging of gravity waves 2. Critical layer filtering. J. Geophys. Res. 106 (D15), 17205–17220.

Suzuki, S., Shiokawa, K., Otsuka, Y., Ogawa, T., Wilkinson, P., 2004. Statistical characteristics of gravity waves observed by an all-sky imager at Darwin, Australia. J. Geophys. Res. 109, D20S07.

Taylor, M.J., Henriksen, K., 1989. Electromagnetic coupling in the Polar clefts and caps. In: Sandholt, P.E., Egeland, A. (Eds.), Springer, New York.

Taylor, M.J., Pendleton Jr., W.R., Clark, S., Takahashi, H., Gobbi, D., Goldberg, R.A., 1997. Image measurements of short-period gravity waves at equatorial latitudes. J. Geophys. Res. 102 (D22), 26283–26299.

Taylor, M.J., Ryan, E.H., Tuan, T.F., Edwards, R., 1993. Evidence of preferential directions for gravity wave propagation due to wind filtering in the middle atmosphere. J. Geophys. Res. 98 (A4), 6047–6057.

Walterscheid, R.L., Hecht, J.H., Vincent, R.A., Reid, I.M., Woithe, J., Hickey, M.P., 1999. Analysis and interpretation of airglow and radar observations of quasi-monochromatic gravity waves in the upper mesosphere and lower thermosphere over Adelaide, Australia (35°S, 138°E). J. Atmos. Sol Terr. Phys. 61, 461–478.

Watanabe, S., Sato, K., Takahashi, M., 2006. A general circulation model study of the orographic gravity waves over Antarctica excited by katabatic winds. J. Geophys. Res. 111, D18104.

Wu, D.L., Jiang, J.H., 2002. MLS observations of atmospheric gravity waves over Antarctica. J. Geophys. Res. 107 (D24), 4773.

Wu, Q., Killeen, T.L., 1996. Seasonal dependence of mesospheric gravity waves (<100 km) at Peach Mountain Observatory, Michigan. Geophys. Res. Lett. 23, 2211–2214.

Yoshiki, M., Sato, K., 2000. A statistical study of gravity waves in the Polar regions based on operational radiosonde data. J. Geophys. Res. 105 (D14), 17995–18011.

Yoshiki, M., Kizu, N., Sato, K., 2004. Energy enhancements of gravity waves in the Antarctic lower stratosphere associated with variations in the polar vortex and tropospheric disturbances. J. Geophys. Res. 109, D23104.